

## Introduction

Planets are formed in the same time when the star form. As we know, the Giant Molecular Clouds (GMC) are dense regions of gas and dust where stars form through accretion processes. Most of the mass in the interstellar medium is grouped into clumps called Giant Molecular Clouds.

Those molecular clouds are known to be rich and nearby forming region star, and therefore ideal laboratories for observational studies. The Composition of material of the GMC is 99% of gas and 1% solid sub-micron particles (dust). Hydrogen is the most elements in the molecular cloud (75 %). Helium is the second most elements with an (25 %), which is then followed by fewer heavier elements such as carbon, nitrogen, calcium, and sodium.

The major component of GMCs is  $H_2$ , but they are detected in the CO line because  $H_2$  cannot be excited at the low temperature of these clouds. CO is the best tracer of the diffuse medium because it is very abundant ( $[CO]/[H_2]$ ,  $\sim 10^{-4}$ ), it has a relatively high dissociation energy (11.09 eV) and it can be excited from millimetre wavelengths (few Kelvin) to the near infrared ( $\sim 3000$  K) in a variety of different physical environments. The nearest molecular clouds to our solar system are *Orion*, *Ophiuchus*, *Taurus-Auriga*, *Chameleon*, and *Serpens*.



**Figure-1-:** Orion nebula was captured by Hubble Space Telescope [HST](#) in 2009. As noticed from the image, Orion consists of gas and dust, many of stars born surrounded by materials.

The number of densities in the Giant Molecular Cloud in the range  $1 \times 10^8 - 3 \times 10^8 \text{ m}^{-3}$  and temperature of approximately 15 k. The size of the clouds is 50 pc in diameter and masses of the clouds are between  $10^5$  and  $10^6 M_{\odot}$ .

The table below shows the summary of values for some molecular clouds.

	<i>Orion Or (M42)</i>	<i>Ophiuchus</i>	<i>Taurus-Auriga</i>	<i>Chameleon</i>	<i>Serpens</i>
<i>Number of density</i>	$3 \times 10^8 \text{ m}^{-3}$	$5 \times 10^9 \text{ m}^{-3}$	$10^9 \text{ m}^{-3}$	-	-
<i>Distance</i>	400 pc	140 pc	140 pc	160 pc	436 pc
<i>Diameter</i>	60 pc	6 pc	2 pc	-	-
<i>Mass</i>	$10^6 M_{\odot}$	$10^4 M_{\odot}$	$50 M_{\odot}$	$5000 M_{\odot}$	$290 M_{\odot}$
<i>Temperature</i>	15 k	50 k	10 k	-	30 k

**EX.1:** How many solar-type stars could be made from a giant molecular cloud of diameter 10 pc and density  $1.6 \times 10^{-17} \text{ Kg/m}^3$ ? Assume the cloud is spherical and about half of it is used to form stars.

**EX.2:** What is the peak wavelength of the emission from cool dust (100 k)?

The collapse of the molecular cloud is started when the mass of the cloud exceeds the Jeans criterion, or Jean's mass. When the gravitational pull overtakes the radiative gas pressure, then the molecular cloud starts to collapse inwardly. The Jeans mass is calculated according to:

$$M_J \approx \left( \frac{5kT}{G\mu m_H} \right)^{3/2} \left( \frac{3}{4\pi\rho_0} \right)^{1/2} \quad (1)$$

where  $k$  is the Boltzmann's Constant ( $k = 1.38 \times 10^{-8} \text{ J k}^{-1}$ ),  $T$  is the temperature of the cloud and  $G$  is the Gravitational Constant ( $G = 6.674 \times 10^{-11} \text{ m}^3/\text{kg}^1 \text{ s}^2$ ),  $\mu$  is the mean molecular weight,  $m_H$  is the mass of the hydrogen atom ( $m_H = 1.6735 \times 10^{-27} \text{ kg}$ ),  $\rho$  is the density of the cloud in unit ( $\text{kg/m}^3$ ).

There are two scenarios of collapse in a giant molecular cloud.

1. The homologous collapse is a scenario where the uniform density across the molecular cloud makes the different regions of the cloud to collapse in about the same amount of time.
2. The inside-out collapse describes a scenario where, if the cloud center is denser than the outer regions, the time of collapse in the center will be shorter. This means the material which is close to the center will require a shorter time to collapse than the material which is far from the center.

The time of cloud collapse is called Free-Fall time-scale and can be determined by:

$$t_{ff} = \left( \frac{3\pi}{32G\rho_0} \right)^{1/2} \quad (2)$$

The Free-Fall time-scale is the time to collapse from original shape to a single point due to gravity, neglecting counter – balancing pressure force.

The inner dense core in the center of the collapse cloud is called **Protostar**. The cloud has non-zero angular momentum; hence any initial rotation of the cloud will cause the in-falling material to build up a disk around the protostar. The phase when the nuclear reactions start inside the core of the star is known as *Zero-Age Main Sequence* (ZAMS) star phase. The time scale for this duration called Kelvin-Helmholtz time scale and can be estimated through this formula:

$$t_{kh} \approx \frac{GM^2}{RL} \quad (3)$$

where  $R$  is the radius of the proto-star and  $L$  is the average luminosity. The time scale ( $t_{kh}$ ) for one solar mass is ( $\approx 4 \times 10^7$  yr).

## Spectral Energy Distributions (SEDs)

**Spectral Energy Distributions** is a graph of the energy emitted by an object as a function of different wavelengths. The graph at figure 2 is a typical curve, called a blackbody curve. It shows that the amount of energy emitted by the object at all wavelengths varies with the temperature of the object. Hotter objects emit more light at shorter wavelengths than cooler objects; therefore the hotter the object, the more the peak wavelength is shifted toward the left of the graph.

Stars aren't really blackbodies but the emission from them is very similar to blackbodies. We can "fit" a blackbody curve to the star. Any emission from dust around the stars will then be really obvious because it will show up as "extra" emission (but at a much lower temperature than the star) because the dust is being warmed up by the star. Sometimes this emission can be fit by another much cooler blackbody.

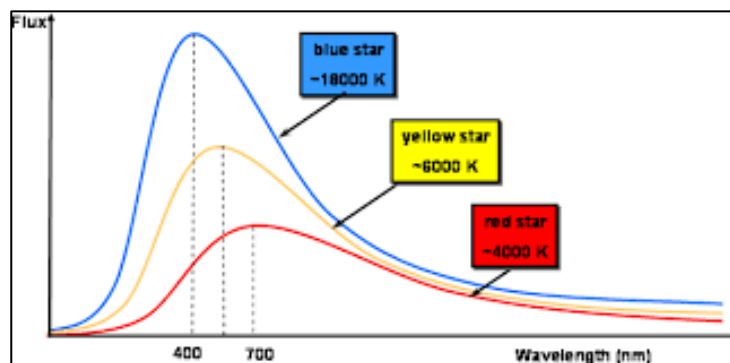


Figure-2-: Represent the relation between the flux and wavelength.

## Young Stellar Objects (YSOs)

Young Stellar Objects in the pre-main sequence phase are classified into four classes according to the observed properties at millimeter, infrared, and optical wavelengths. This classification based on the Spectral Energy Distribution (SED) shape. SEDs were found to have different shapes classification association with YSOs evolution. The origin of SED emission of the YSOs comes from two

components. The first component is the protostar which emits as a black body radiation in the SED and the second component is the thermal emission comes mainly from the dust in the protoplanetary disk.

For more clarification, the material closest to the protostar can be emitted in the Near-Infrared (NIR) wavelengths range (0.7  $\mu\text{m}$  - 5  $\mu\text{m}$ ), material a little farther would emit in the Mid-Infrared (MIR) wavelengths range between (5  $\mu\text{m}$  - 20  $\mu\text{m}$ ) and for material more farther distance from the protostar are colder and emit in the Far-Infrared (FIR) wavelengths range (20  $\mu\text{m}$  - 1 mm), sub-millimeter wavelengths.

The classifications can be extracted from the slope of the SED by using this formula:

$$\alpha \approx \frac{d \log(\lambda F_{\lambda})}{d \log \lambda} \quad (4)$$

Where  $\lambda$  is the wavelength and  $F_{\lambda}$  is the observed flux.

**Class 0:** It represents the earlier stage of young stellar objects formation. It was not found in the first classification from Lada (1987), but it was added later by Andre et al. (1993). In this class, protostar forming is embedded by accreting an envelope and has a very strong emission in the sub-millimeter wavelength and it is not visible in the optical. Some objects can be observed in the MIR and FIR.

**Class I ( $\alpha > 0$ ):** When the value of the slope is positive. Young stellar objects are forming a star with very strong outflows or called (bipolar jets) and surrounded by the protoplanetary disk. The envelope in this stage starts to dissipate and a star becomes partially observed in the optical. The SED has a rising in the MIR emission which mostly comes from the protoplanetary disk.

**Class II ( $-1.5 < \alpha < 0$ ):** The star in this class is called Pre-Main sequence star. Where most of the materials in the envelope have been dissipated and the star becomes observed completely in the optical wavelength. The SED of Class II has combined emission from the star and the disk and has a very less strong Infrared (IR)-emission from Class 0 and I. This emission comes from the dust and the gas in the protoplanetary disk.

The protostars in this class can be divided into three types according to their masses. Pre-Main-Sequence stars with masses less than  $2 M_{\odot}$  are called Low Mass Stars. Low Mass Stars are classified to Classical T-Tauri Stars (CTTs) and Weak T-Tauri Stars (WTTs) which has weaker IR emission than CTTs. The protostar has mass larger than  $2 M_{\odot}$  or in the range ( $2 M_{\odot} - 8 M_{\odot}$ ) known as Intermediate Mass Stars “Herbig Ae/Be stars”, as shown in Figure 2.

Massive stars protostars which have masses greater than ( $8 M_{\odot} - 10 M_{\odot}$ ) are called “Massive stars”. The massive stars cannot be observed during Class II because they are evolved much quicker than low mass stars.

**Class III ( $\alpha < 0$ ):** The young stellar object reaches to the stage of the main sequence stars and the disk around the star is called “Debris Disk”. The SED of the Class III stage has less IR emission and the debris disk is optically thin. The reason behind the IR emission of the SED in Class III is less than Class II due to use of all dust and gas in the protoplanetary disk to form planets. This small IR emission originates from the collision of the giant planets with residual small grains, comets, planetesimals. The sketch below show the young stellar object evolution through four Classes with time.

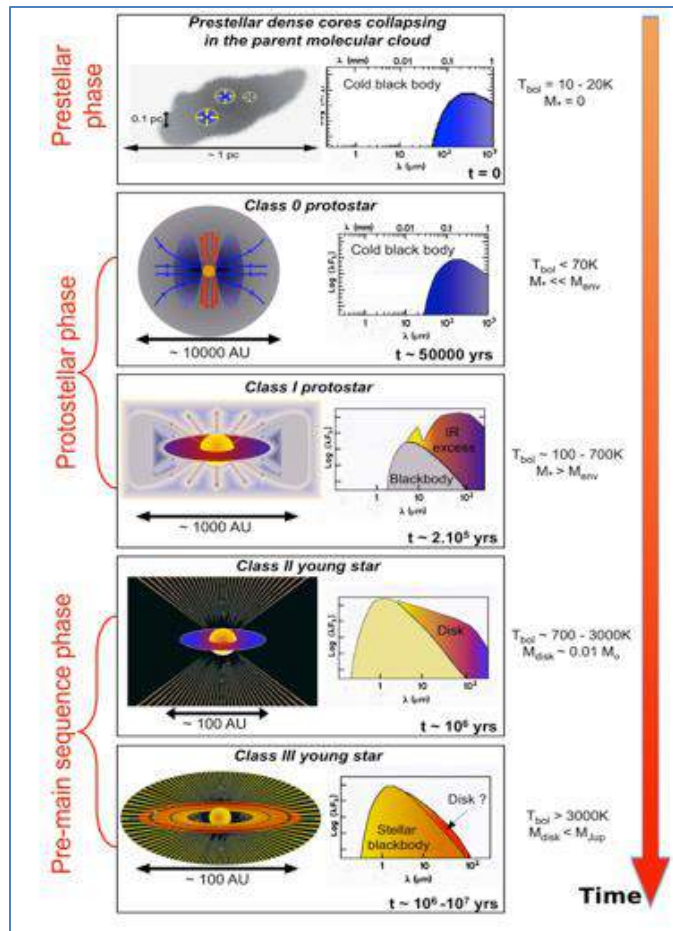


**Figure-3-:** Scheme to show Infrared emission in spectral energy distribution changes with young stellar objects evolution.

## Protoplanetary Disk

Protoplanetary disks are large reservoirs of dust and gas, are mostly formed of molecular hydrogen gas (~99 % of the disk's mass) and of dust particles (~1 % of the disk's mass). They are evidenced to be the birthplace of exoplanets, which form out of the disk material. This primordial disk, which is a byproduct of star formation, is typically detected in the Class II phase, more rarely in the Class I phase (see Figure 3).

For low- and intermediate-mass pre-main sequence stars, this is in part due to the fact that the object spends a longer lifetime ( $10^6 - 10^7$  yr) in the Class II phase than in the Class I phase ( $10^5$  yr).

Observations of young stellar objects and T Tauri stars in particular are generally done at sub-millimeter and infrared wavelengths. If we plot the spectral energy distribution of young stellar objects, we find that there is excess infrared emission.

Therefore, there are two types of the typically foreseen for protoplanetary disks:

1. **Passive Disk** is irradiated disk absorbs the stellar photons of the central star and re-emits the light at infrared wavelengths, depending on the opacity of the disk's dust.
2. **Active disk** is emission produce from a friction between the gas molecules or dust particles of the disk.

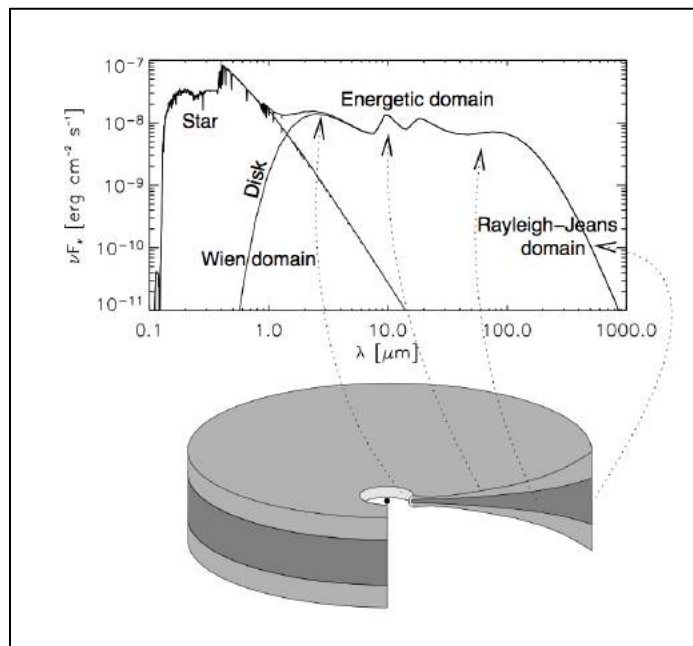
Protoplanetary disks are observed around pre-main sequence (PMS) stars, before the start of the nuclear reactions in the stellar core. Based on their mass, PMS stars are classified as T-Tauri stars ( $< 2 M_{\odot}$ ) and Herbig stars (between 2 and  $10 M_{\odot}$ ). Disks have also been observed around brown-dwarfs and even around planetary-mass objects.

While the model of formation of high-mass stars theorized the low-probability of disk survival around stars more massive than  $10 M_{\odot}$  on time scales longer than  $10^5$

years, observational evidence of this transient phase was revealed by high-angular resolution observation.

The highly complex structure of a protoplanetary disk results from different physical properties in different regions of the disk. One of the first and powerful method to study pre-main sequence objects is through the analysis of the SED, as illustrated in Figure 4.

The figure 4 shows a sketch of protoplanetary disk. The central star dominates the emission at optical wavelengths ( $\lambda \leq 1 \mu\text{m}$ ). The inner disk ( $T \sim 1500 \text{ K}$ ) can be observed at near-infrared wavelengths ( $1 \leq \lambda \leq 5 \mu\text{m}$ ). The surface of the disk ( $T \sim 100 - 500 \text{ K}$ ) is best studied at mid-infrared wavelengths ( $5 \leq \lambda \leq 50 \mu\text{m}$ ). The colder ( $T \sim 100 \text{ K}$ ) outer parts of the disk are observed though observations in the far-infrared up to millimeter wavelengths ( $1 \text{ \& } 50 \mu\text{m}$ ). Not shown on this SED is that accretion columns and/or accretion spots on the star can have temperatures of  $\sim 10^4 \text{ K}$  or more leading to an excess at ultraviolet wavelengths.



**The figure 4:-** Shows a sketch of protoplanetary disk and SED shape for pre-main-sequence star with protoplanetary disk.

## **Observations of disk evolution:**

In 1983, the Infrared Astronomical Satellite (IRAS) was the first space telescope to perform a survey of the entire sky at infrared wavelengths.

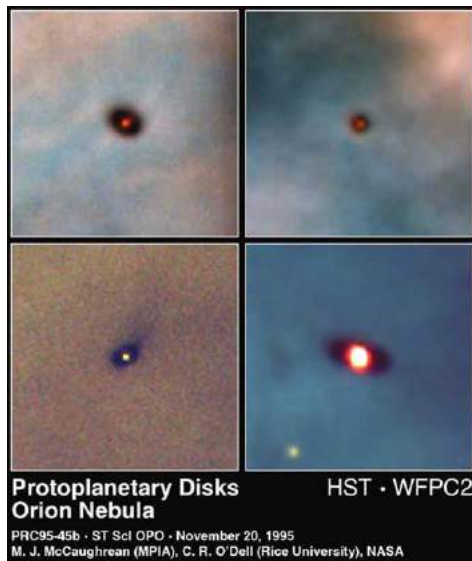
IRAS triggered the first systematic studies on the variety of SEDs of protoplanetary disks. Follow-up space based infrared telescopes further opened up of the infrared sky, improving in spatial and spectral resolution and sensitivity.

In 1995, the Infrared Space Observatory (ISO) was the first to reveal the incredible richness of the mid-IR spectrum. Most notably, the characteristic emission features from polycyclic aromatic hydrocarbon (PAH) and silicate dust grains could be studied in detail. The analysis of these spectral features provides insight into the physical processes in disks. Less than a decade later, ISO was followed up in 2003 by the Spitzer Space Observatory. Spitzer improved the infrared view of protoplanetary disks.

On May, 14, 2009, the next space telescope was launched towards its operational orbit: Herschel. Three instruments on board of Herschel performed imaging photometry and spectroscopy in the far-infrared and sub-millimeter part of the spectrum (55–672  $\mu\text{m}$ ). Herschel provided the spectral resolution and sensitivity to study the spectral features at 69  $\mu\text{m}$  from crystallised silicate dust grain. The James Webb Space Telescope (JWST) and the Space Infrared Telescope for Cosmology and Astrophysics (SPICA) are the next telescopes capable of observing at infrared wavelengths, and are scheduled to be launched in 2018 (change to 2022) and 2025 respectively.

JWST and SPICA have even larger mirrors and more sensitive instruments which will provide unprecedented resolution and sensitivity from the near- to far-infrared.

Evidence for primordial disks is essentially completely absent for stars of age 10 Myr or above. From these observations, one infers a disk lifetime of about 3–5 Myr.



**The figure 5:-** Protoplanetary disks observed by the HST 1995 (image credit: courtesy NASA, ESA)

Protoplanetary disks are optically thick and can be detected or observed by different techniques, which include:

1. Detection of infrared excesses in the near- or mid-IR. The excess indicates the presence of warm dust close to the star.
2. Detection of an accretion signature indicative of gas being accreted on to the star. Observational indicators include an ultraviolet excess,  $H_{\alpha}$  emission with a large equivalent width, and a number of other emission lines such as the Ca II triplet in the infrared.
3. Observation of mm or sub-mm flux arising from cool dust in the outer disk.
4. Disk imaging, either in scattered visible light from the central star, or in silhouette against a bright background nebula.
5. Detection of line emission from molecular species such as CO or  $NH_3$ ,

## Disk Structure

The population of protoplanetary disks is observed to evolve, but the dominant physical processes responsible for this evolution remain unclear.

The few Myr lifetimes of protoplanetary disks equates to millions of dynamical times in the inner disk and thousands of dynamical times in the outer disk at 100 AU. To a first approximation we can treat the disk as evolving slowly through a sequence of axisymmetric static structures as mass accretes on to the star and is lost through disk winds, and our first task is to discuss the physics that determines those structures.

Quantities that we are interested in include the density  $\rho(r, z)$ , the gas and dust temperatures  $T(r, z)$  and  $T_d(r, z)$ , the chemical composition, and the ionization fraction.

The density of solid particles (“dust”)  $\rho_d$  is also important, but we will defer saying much about that until we have discussed turbulence, radial drift, and the aerodynamic coupling of solids and gas.

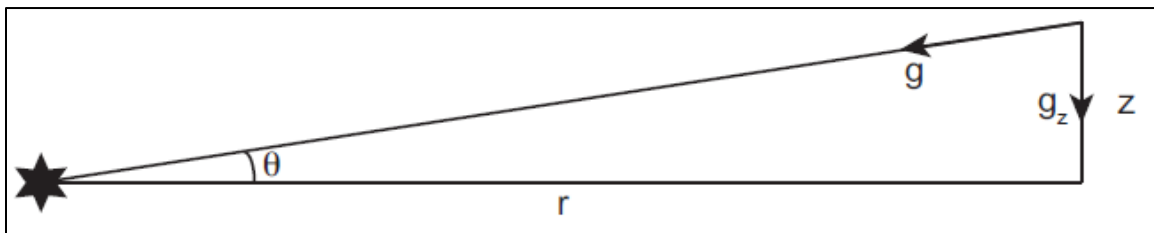


**Figure - 6-:** The geometry for calculating the vertical hydrostatic equilibrium of a non-self-gravitating protoplanetary disk. The balancing forces are the vertical component of stellar gravity and the vertical pressure gradient.

### 1.Vertical Structure:

Protoplanetary disks are flared with a vertical scale height that increases with radius. Kenyon & Hartmann (1987) first suggested the possibility of flaring

based on the large far-IR excesses detected by IRAS that could not be explained by a spatially flat disk

We can derive the structure of the disk using the principle of hydrostatic equilibrium. We will examine the balance between pressure and gravity for the small element of the disk as shown in figure 6, where:

$$dP = -g \rho dz \quad \text{-----(1)}$$

where  $P$  is the pressure depends on the height above the surface ( $z$ ),  $\rho$  is the density,  $g$  gravity force and  $dz$  scale height.

The relation between the density of the gas in the disk and scale height of the disk can be written:

$$\rho = P \mu_A m_{\text{amu}} / kT \quad \text{-----(2)}$$

where  $\mu_A$  is the mean molecular weight of the gas in the disk,  $m_{\text{amu}}$  is the atomic mass unit,  $k$  is Boltzmann's constant,  $T$  the absolute temperature.

We can combine the two equations (1) and (2) to obtain the following:

$$\frac{dP}{dz} = -\frac{P \langle \mu_A \rangle m_{\text{amu}} g}{kT} \quad \text{-----(3)}$$

The negative sign arises because the pressure must decrease in the direction of increasing  $z$  for the gravitational and pressure forces to balance.

The differential equation (3) can be solved by integrating this equation.

$$P = P_0 e^{-\left(\frac{\langle \mu_A \rangle m_{\text{amu}} g z}{kT}\right)} \quad \text{-----(4)}$$

Then

$$P = P_0 e^{-\frac{z^2}{H^2}} \quad \text{-----(5)}$$

in which  $P_0$  is the pressure at the surface at  $z = 0$ , the mid-plane of the disk.

We will only consider forces in the vertical direction and we will assume the Sun has already formed in the center of the disk and that all the gravitational force in

the element is produced by the sun, which is reasonable because the mass of the Sun is 99.9 % of the total mass of the solar system.

Form figure 6. a small element in the protoplanetary nebula,  $r$  is the distance from of the element along the disk,  $Z$  is its distance in the vertical direction from mid-plane of the disk.

The gravitational force on the element is:

$$F_g = \frac{GM_{\odot}\rho A\delta z}{a^2} \text{ -----(6)}$$

Where  $A$  is the cross-sectional area of the element,  $\delta z$  is its thickness and  $\rho$  is the density of the gas it contains. We will assume the angle  $\theta$  is very small, so  $a \approx r$  and  $\sin(\theta) \approx z/a \approx z/r$ . The vertical component of the gravitational force is therefore:

$$F_g = \frac{GM_{\odot}\rho A z \delta z}{r^3} \text{ -----(7)}$$

From equation (7) ,(5) and (4) the scale height of the disk structure  $H$  is given by:

$$H = \sqrt{\frac{2r^3kT}{\langle\mu_A\rangle m_{\text{amu}} GM_{\odot}}} \text{ -----(8)}$$

$H$  is the scale height of the disc, the height at which the pressure has fallen by a factor of  $e^{-1}$ . The equation shows that the thickness of the disc increases with increasing distance from the Sun.

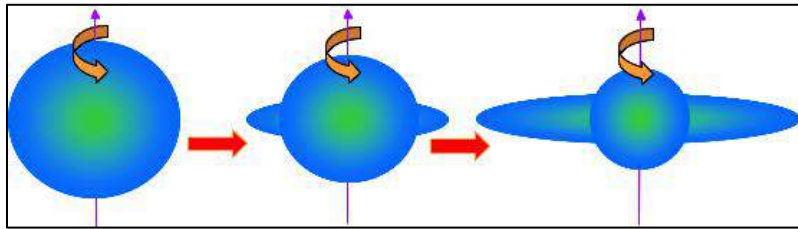
## **2. Disk Velocity:**

Protoplanetary disks form as a natural consequence of cloud collapse due to angular momentum conservation. Angular momentum is given by:

$$\vec{L} = m \vec{r} \times \vec{v} \text{ -----(1)}$$

So as the cloud contracts,  $r$  gets smaller thus  $v$  must increase and so the cloud spins faster. This rapid rotation creates large centrifugal forces. These centrifugal forces

are greatest at the equator and the rotating contracting cloud starts to spread out and form a disk as shown in figure 7.



**The figure 7:-** Shows a centrifugal forces work to create the of protoplanetary disk around of pre-main-sequence star.

The gas in the disk is in Keplerian rotation, the collision velocity increases from the outer to the inner regions; therefore the dynamical timescale is shorter for the inner disk in comparison to the outer disk.

For a geometrically thin, low-mass disk, the deviation from a point-mass Keplerian rotation curve is small and the specific angular momentum.

We can derive useful results for the azimuthal velocity  $v_\phi$ . If the disk is static (and even if it is slowly evolving) the azimuthal component of the momentum equation can be obtained using the Euler equation of conservation of momentum for flow:

$$\frac{\partial \mathbf{v}}{\partial t} + (\mathbf{v} \cdot \nabla) \mathbf{v} = -\frac{1}{\rho} \nabla P - \nabla \Phi \quad \text{-----(2)}$$

where  $\mathbf{v}$  is the velocity and  $\Phi$  is the gravitational potential. Assuming a stationary flow,  $\partial \mathbf{v} / \partial t = 0$ ; that the gravitational potential is dominated by the star; considering cylindrical coordinates; and assuming an axisymmetric flow, so that all the components of Equation 2, can be written in the mid-plane as,

$$\frac{v_\phi^2}{r} = \frac{GM_*}{r^2} + \frac{1}{\rho} \frac{dP}{dr}. \quad \text{-----(3)}$$

Here  $P$  is the pressure and all quantities are mid-plane values. Let's start with an explicit example of the consequences of this force balance in protoplanetary disks.

The Keplerian speed is given by  $v_K = \Omega_K r$ , therefore,

$$v_\phi = \sqrt{v_K^2 + \frac{r}{\rho} \frac{dp}{dr}}. \text{-----(4)}$$

Consider a disk with  $\Sigma \propto r^{-1}$  and central temperature  $T_c \propto r^{-1/2}$ . We then have the sound speed  $c_s \propto r^{-1/4}$ , the density  $\rho \propto r^{-9/4}$  and the pressure  $P \propto r^{-11/4}$ . Substituting into Eq. (3) yields,

$$v_\phi = v_K \left[ 1 - \frac{11}{4} \left( \frac{h}{r} \right)^2 \right]^{1/2} \text{-----(5)}$$

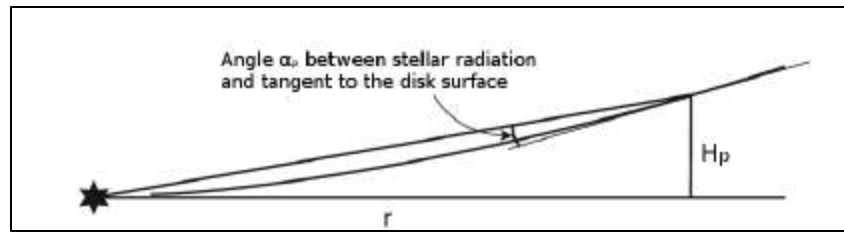
The pressure near the mid-plane usually decreases with radius, thus  $dp/dr < 0$ , indicating that the flow is sub-Keplerian. If the disk density and temperature structures are known and assuming an equation of state, one can determine the fluid azimuthal velocity by using Equation 5.

### 3. Temperature

The temperature structure can be set by the balance between cooling and heating. The two main sources of heating are accretion and reprocessing of stellar radiation by dust grains. The cooling comes basically from dust emission.

Considering a flared disk, the temperature profile can be derived by evaluating how much stellar radiation can be intercepted by the disk surface at a position  $r$  and height  $H_p$  above the mid-plane, Figure 5 shows the geometry considered.

Assuming that the star is a point source and that the disk surface can see all the stellar surface. The rate of heating per unit disk area can be estimated by the stellar flux absorbed at a distance  $r$  and a height  $H_p$



**The figure 8:-** This sketch shows the geometry of a flared disk, with the important parameters to estimate the temperature profile. The radiation of the star is absorbed at a distance  $r$  and height  $H_p$  above the mid-plane. The angle  $\alpha_p$  between the stellar radiation and the tangent to the disk surface is also shown in figure.

The temperature structure can be obtained by imposing the balance between heating and cooling:

$$T(r) = \left( \frac{L_\star}{4\pi\sigma} \right)^{1/4} \alpha_p^{1/4} r^{-1/2}$$

$$T(r) = \left( \frac{R_\star}{r} \right)^{1/2} \alpha_p^{1/4} T_\star, \quad \text{-----(6)}$$

with the stellar luminosity given by:

$$L_\star = 4\pi R_\star^2 \sigma T_\star^4, \quad \text{-----(7)}$$

where  $R_\star$  is the stellar radius and  $T_\star$  is the effective stellar temperature.

The angle  $\alpha_p$  is given by:

$$\alpha_p \simeq 0.4 \frac{R_\star}{r} + r \frac{d(H_p/r)}{dr} \quad \text{-----(8)}$$

#### 4. Density:

An expression for the vertical structure of the density can be obtained, assuming that the disk is in vertically hydrostatic equilibrium, so that:

$$\frac{dp}{dz} + \rho g_z = 0, \quad \text{-----(1)}$$

where  $p$  is the pressure,  $\rho$  is the density, and  $g_z$  is the vertical acceleration. In order to relate pressure with density, an ideal equation of state is considered

$$p = c_s^2 \rho, \quad \text{-----(2)}$$

where  $c_s$  is the sound speed and the disk is assumed to be vertically isothermal, so that  $c_s$  does not depend on  $z$ . Now, it is needed to obtain the gravitational vertical acceleration.

Considering that the disk mass is much smaller than the stellar mass, so that self-gravity can be neglected, a reasonable assumption for disks with masses up to  $\sim 0.1M_\odot$ . The disk, then, just feels the gravitational force from the star, thus

$$g_z = g \sin \theta = \frac{GM_\star}{(r^2 + z^2)} \frac{z}{\sqrt{(r^2 + z^2)}} \quad \text{-----(3)}$$

where  $r$  is the cylindrical disk radius,  $z$  is the disk height above the mid-plane,  $g$  is the gravitational acceleration,  $\theta$  is the angle from  $r$  to  $z$ ,  $G$  is the gravitational constant, and  $M_\star$  is the stellar mass. Using Equations 1 and 2, Equation 3.

$$\frac{d\rho}{\rho} = -\frac{GM_\star z}{c_s^2 (r^2 + z^2)^{3/2}} dz \quad \text{-----(4)}$$

The integration of Equation 4 gives the solution

$$\rho(r, z) = C \exp\left(\frac{GM_\star}{c_s^2 \sqrt{r^2 + z^2}}\right) \quad \text{-----(5)}$$

where  $C$  is the integration constant and can be defined, for instance, by the mid-plane density at the inner disk radius.

Due to the large surface areas, Protoplanetary disk can cool down very efficiently. Thus, their temperature and pressure are very low. One then need to assume that the disk is thin, meaning that the vertical extent is much smaller than the radial extent ( $z \ll r$ ). Otherwise, pressure would not be able to counteract gravity and all the matter would fall in to the central star. Under the supposition that  $z \ll r$ , the below function can be Taylor expanded:

$$(r^2 + z^2)^{-1/2} \simeq \frac{1}{r} - \frac{z^2}{2r^3} \quad \text{-----(6)}$$

The Keplerian angular velocity is given by:

$$\Omega_K = \sqrt{\left(\frac{GM_\star}{r^3}\right)}. \quad \text{-----(7)}$$

Therefore, Equation (1) can be written as:

$$\rho(z) = \rho(r) \exp\left(-\frac{z^2}{2H^2}\right) \quad \text{-----(8)}$$

where  $\rho(r)$  is the mid-plane density and the disk scale height is defined as

$$H \equiv \frac{c_s}{\Omega_K}. \quad \text{-----(9)}$$

The radial structure of the density cannot be derived without knowing the nature of angular momentum transport or using observational constraints, but it is often parameterized as a power law of radius:

$$\rho(r) \propto r^{-\delta} \quad \text{-----(10)}$$

Typical values for the power law are  $\delta = 1.0$  or  $\delta = 1.5$ .

## **Turbulence:**

Turbulence in the protoplanetary disks is important for two independent reasons.

**First**, it could account for disk evolution by redistributing angular momentum much faster than molecular viscosity.

**Second**, turbulence has increase of planet formation processes, ranging from the collision velocities of small particles to the formation of planetesimals and the migration rate of low-mass planets.

Here lists some of the possible sources of turbulence:

### **1. Hydrodynamic Turbulence**

The temperature varies with radius, giving rise both to vertical shear and qualitatively distinct possibilities for instability.

## 2. Self-gravity

A disk is described as self-gravitating if it is unstable to the growth of surface density perturbations when the gravitational force between different fluid elements in the disk is included along with the force from the central star.

## 3. Magnetohydrodynamic Turbulence

This is the magneto rotational instability (MRI) which is accepted as the dominant source of turbulence in well-ionized accretion disks (winds could still contribute to or dominate angular momentum loss).

## Episodic accretion

Young stellar objects (YSOs) are observed to be variable. The short time scale (lasting hours to weeks) component of that variability is complex, but can probably be explained as a combination of turbulent inhomogeneities in the inner disk, stellar rotation, and the complex dynamics of magnetospheric accretion.

There is also longer time scale variability — lasting from years to (at least) many decades, that in some cases takes the form of well-defined outbursts in which the YSO brightens dramatically.

## Single Particle Evolution

The evolution of solid particles within disks differs from that of gas because solid bodies are unaffected by pressure gradients but do experience aerodynamic forces.

## Ice Lines and radial Structure

The water snow line, together with the silicate sublimation front and various ice lines in the outer disk, are potentially critical locations for planet formation. Inside the snow line, water exists in the gaseous phase, though it dissociates at  $T > 2500$  K.

As water vapor interior to the ice line diffuses past the snow line, it condenses into icy grains. The snow line thus acts as a cold trap, where the enhanced mass in water ice, should accelerate the growth of planetesimals and perhaps gas giant planets.

Water is abundant throughout the Solar System. Outside of the Earth, water appears in spectra of comets, Kuiper belt objects, and satellites of giant planets (including the Moon) and bound within minerals on Mars, Europa, and some asteroids.

Because they can be analyzed in great detail, meteorites from asteroids provide a wealth of information on water in the inner Solar System.

The water content of Solar System bodies helps trace the evolution of the snow line. Ice on the Earth and on Mars suggests the possibility that the snow line might have been as close as 1 AU to the proto-Sun, a real possibility for passively irradiated disks.

## **Disk Dispersal:**

Different mechanisms can be explained the dispersal of the circumstellar material in protoplanetary disks:

- 1. Photo-evaporation:** is a purely hydrodynamic process that occurs when molecular gas in the disk is dissociated or ionized by high energy (**UV** or **X-ray**) photons.

Photoevaporation can be driven by energetic photons in the far-ultraviolet (FUV:  $6 \text{ eV} < h\nu < 13.6 \text{ eV}$ ), extreme-ultraviolet (EUV:  $13.6 \text{ eV} < h\nu < 0.1 \text{ keV}$ ) and X-ray ( $h\nu > 0.1 \text{ keV}$ ) energy range. Photons in each energy range affect the disks in different ways, and the relative importance of FUV, EUV, and X-ray photoevaporation is still not well understood. Photoevaporating photons can originate both from nearby massive stars and from the central star itself.

Photo-evaporation results, for instance, onto the formation of a gap that separates the inner and outer disk regions. Photoevaporation removes all circumstellar gas very quickly ( $<1$  Myr) once accretion stop. Where the direct irradiation of the gas by UV photons results in an increase of the gas temperature, and consequently in an increase of the thermal velocity ( $v_{\text{th}}$ ) of the gas.

**2. Grain growth and dust settling:** Even though solid particles only represent 1% of the initial mass of the disk, understanding their evolution is of the most interest for disk evolution and planet formation studies.

Small ( $r \sim 0.1 \mu\text{m}$ ) grains have a large surface-to-mass ratio and are swept along with the gas. As grains collide and stick together, their surface-to mass ratio decreases and their motions decouple from the gas. They therefore suffer a strong drag force and settle toward the mid-plane.

At the same time, grains grow into larger bodies that settle onto the mid-plane of the disk where they can grow into rocks, planetesimals and beyond.

The formation of planets is a second scenario classically can explain the disk dispersal.

Rapid grain growth and gas accretion onto the forming planetesimals can disperse the disk in few Myr. This timescale also depends on different factors such as the stellar mass and the grain opacity.

## **Turbulence:**

Turbulence in the protoplanetary disks is important for two independent reasons.

**First**, it could account for disk evolution by redistributing angular momentum much faster than molecular viscosity.

**Second**, turbulence has increase of planet formation processes, ranging from the collision velocities of small particles to the formation of planetesimals and the migration rate of low-mass planets.

Here lists some of the possible sources of turbulence:

1. **Hydrodynamic Turbulence**

The temperature varies with radius, giving rise both to vertical shear and qualitatively distinct possibilities for instability.

2. **Self-gravity**

A disk is described as self-gravitating if it is unstable to the growth of surface density perturbations when the gravitational force between different fluid elements in the disk is included along with the force from the central star.

3. **Magnetohydrodynamic Turbulence**

This is the magneto rotational instability (MRI) which is accepted as the dominant source of turbulence in well-ionized accretion disks (winds could still contribute to or dominate angular momentum loss).

## **Episodic accretion**

Young stellar objects (YSOs) are observed to be variable. The short time scale (lasting hours to weeks) component of that variability is complex, but can probably be explained as a combination of turbulent inhomogeneities in the inner disk, stellar rotation, and the complex dynamics of magnetospheric accretion.

There is also longer time scale variability — lasting from years to (at least) many decades, that in some cases takes the form of well-defined outbursts in which the YSO brightens dramatically.

## **Single Particle Evolution**

The evolution of solid particles within disks differs from that of gas because solid bodies are unaffected by pressure gradients but do experience aerodynamic forces.

## **Ice Lines and radial Structure**

The water snow line, together with the silicate sublimation front and various ice lines in the outer disk, are potentially critical locations for planet formation. Inside the snow line, water exists in the gaseous phase, though it dissociates at  $T > 2500$  K.

As water vapor interior to the ice line diffuses past the snow line, it condenses into icy grains. The snow line thus acts as a cold trap, where the enhanced mass in water ice, should accelerate the growth of planetesimals and perhaps gas giant planets.

Water is abundant throughout the Solar System. Outside of the Earth, water appears in spectra of comets, Kuiper belt objects, and satellites of giant planets (including the Moon) and bound within minerals on Mars, Europa, and some asteroids.

Because they can be analyzed in great detail, meteorites from asteroids provide a wealth of information on water in the inner Solar System.

The water content of Solar System bodies helps trace the evolution of the snow line. Ice on the Earth and on Mars suggests the possibility that the snow line might have been as close as 1 AU to the proto-Sun, a real possibility for passively irradiated disks.

## Disk Dispersal:

Different mechanisms can be explained the dispersal of the circumstellar material in protoplanetary disks:

- 1. Photo-evaporation:** is a purely hydrodynamic process that occurs when molecular gas in the disk is dissociated or ionized by high energy (**UV** or **X-ray**) photons.

Photoevaporation can be driven by energetic photons in the far-ultraviolet (FUV:  $6 \text{ eV} < h\nu < 13.6 \text{ eV}$ ), extreme-ultraviolet (EUV:  $13.6 \text{ eV} < h\nu < 0.1 \text{ keV}$ ) and X-ray ( $h\nu > 0.1 \text{ keV}$ ) energy range. Photons in each energy range affect the disks in different ways, and the relative importance of FUV, EUV, and X-ray photoevaporation is still not well understood. Photoevaporating photons can originate both from nearby massive stars and from the central star itself.

Photo-evaporation results, for instance, onto the formation of a gap that separates the inner and outer disk regions. Photoevaporation removes all circumstellar gas very quickly ( $< 1 \text{ Myr}$ ) once accretion stop. Where the direct irradiation of the gas by UV photons results in an increase of the gas temperature, and consequently in an increase of the thermal velocity ( $v_{\text{th}}$ ) of the gas.

- 2. Grain growth and dust settling:** Even though solid particles only represent 1% of the initial mass of the disk, understanding their evolution is of the most interest for disk evolution and planet formation studies.

Small ( $r \sim 0.1 \mu\text{m}$ ) grains have a large surface-to-mass ratio and are swept along with the gas. As grains collide and stick together, their surface-to mass ratio decreases and their motions decouple from the gas. They therefore suffer a strong drag force and settle toward the mid-plane.

At the same time, grains grow into larger bodies that settle onto the mid-plane of the disk where they can grow into rocks, planetesimals and beyond.

## Debris Disk

It is established that debris disks consist of second-generation dust that does not come from the protoplanetary-disk phase. These second generation “debris” disks result in a modest but detectable infrared excess, which level declines with increasing age of the system.

This can be explained by the fact that the lifetime for the dust grains to be removed via radiation pressure and Poynting-Robertson drag is much shorter than the age of the system. Therefore, exozodiacal dust must then be regenerated by mechanisms such as collisions between planetesimals or cometary activity.

Most main sequence stars are found to be surrounded by those debris disks. Two noticeable debris disk components in our solar system are the asteroid belt in the terrestrial planet region between 2 AU and 3.5 AU, and the Edgeworth-Kuiper Belt (EKB) which contains the coldest dust at distances larger than 30 AU from the Sun, as shown in Figure 2.7.

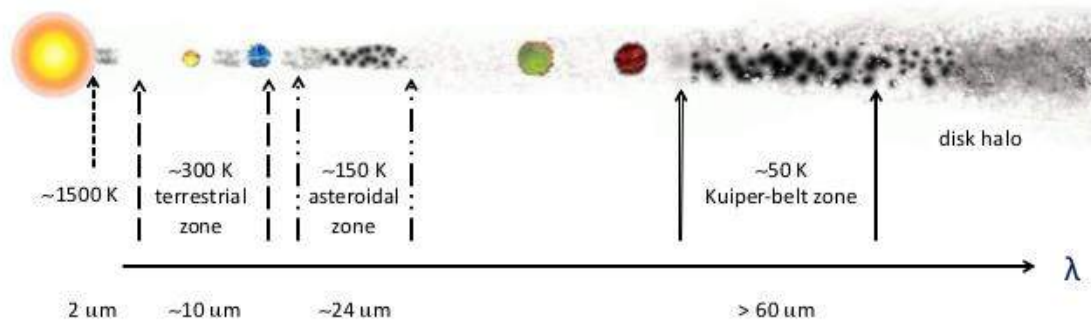


**Figure - 5-:** Dust emission on the debris disks with different wavelengths with typical temperature and regions from the star.

Observationally, the first evidence of debris disks was obtained by Aumann et al. (1984) using the Infrared Astronomical Satellite (IRAS). Aumann et al. (1984) detected a strong infrared excess at 25  $\mu\text{m}$ , 60  $\mu\text{m}$  and 100  $\mu\text{m}$  almost ten times larger than the photospheric flux, which they attributed to cold and solid

material orbiting the star. This discovery led to the expression of “Vega phenomenon” to describe debris disk-like observational properties. Further work by the IRAS investigators team led to the identification and confirmation of four debris disk stars, namely Vega (also known as Alpha Lyr), Fomalhaut, Beta Pictoris and Epsilon Eridani, as shown in Figure 5.

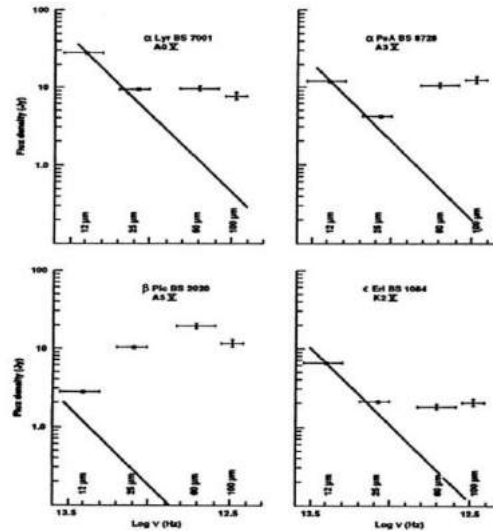


**Figure - 6-:** The Spectral Energy Distribution for Vega, Fomalhaut, Beta Pictoris and Epsilon Eridani from IRAS data.

The first image of a debris disk was of light scattered by a dust disk around the nearby main-sequence star  $\beta$  Pictoris and the image is taken 1984 using optical telescope.

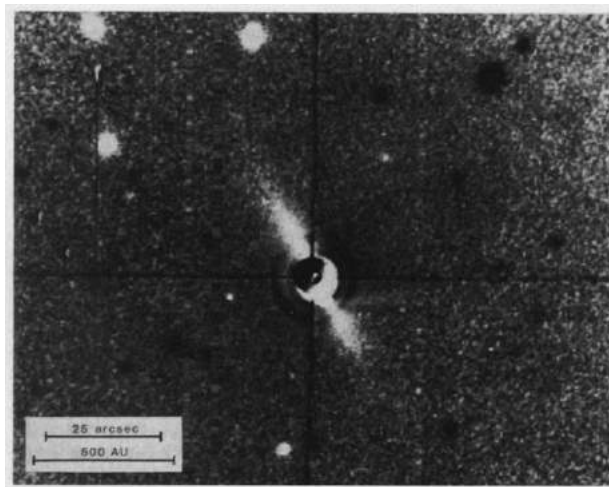


**Figure - 6-:** The left image is taken 1984 using optical telescope for Beta Pictoris star with debris disk.

**Debris disk properties:**

1. Debris disks are significantly less massive than PMS protoplanetary disks.
2. Optically thin at practically all wavelengths, their total mass can be directly and reliably estimated in the infrared spectral range.
3. The mass in the debris disk is decreased with increasing age of the system.
4. Debris Disk around younger stars have stronger infrared excess and higher fractional luminosity than older main-sequence stars.
5. Debris disk excess around A-type stars for ages between 5 and 850 Myr.
6. Debris Disk around Sun-like stars of spectral type F, G, K, It is found that about 15% of the stars younger than 300 Myr exhibit an infrared excess at 24  $\mu\text{m}$  whereas the rate falls to 2.7% for older ages.
7. Debris Disk around M dwarf star could be detected in the age range of 20 to 200 Myr.

**Planet Formation**

The first large solid objects to form out of the protoplanetary nebula were planetesimals, which had sizes up to about 100km in diameter; gravity then caused these planetesimals to eventually merge to form the planets.

Planet formation starts in the circumstellar disk during the pre-main sequence phase of the young star. Two models are proposed to explain the formation of giant planets in disks:

1. The “core-accretion model”, Pollack et al. (1996) suggests that a protoplanet core forms out from solid elements, which then triggers a second phase where gas from the disk is rapidly accreted by the rocky core.
2. The “disk instability model”, Boss (2006) proposes that marginally stable disks may actually fragment into dense clumps that would become giant planets.

There are two important process works to form planets in the disk. **First process** is the dust particles can stick together and grow into larger planetesimals, where the Van Der Waals forces act to stack the dust particles gradually with each other and to form clumps of crowded particles. This process leads the gas and the solid particles to slowly split up from each other. As a result, the gas remains in hydrostatic equilibrium whereas the solid particles begin to grow and sink toward the mid-plane due to the vertical gravity component.

The sinking speed of the dust grain under the influence of gravity is limited by two factors: the viscosity of the gas and the size of the grain. The possibility of collision with other grains is increased, leading to a corresponding increase in size of the grains and an increasingly faster fall towards the mid-plane, similar to “a snowball rolling down from the iceberg”.

**The second process** involved considers the differential velocity between the gas and the dust grains in rotation around the central star, which leads to a partial decoupling between these two constituents.

Several scenarios of planetesimal evolution are under study, which depend on the amplitude of the mutual gravitational forces between them and cause continuous collisions.

1. Two planetesimals may encounter and bounce back.
2. Two planetesimals may merge and form a larger planetesimal.
3. One or two planetesimals might be chopped into smaller corpses.

The sequence of collisions between small and large planetesimals mostly result in merging. A planetary embryo in the inner region of a protoplanetary disk will stop growing when most dust particles have been accreted. At a distance of about 1 AU, such planetary embryos stop growing once they have reached a mass of about six times the mass of the Moon. For the giant outer planets, the formation scenario first involved the formation of a  $\sim 10 M_{\oplus}$  core, which then quickly accretes the surrounding gas in the protoplanetary disk.